

Light thermal dark matter models in the light of DAMIC-M 2025 constraints

Debasish Borah,^{1,*} Satyabrata Mahapatra,^{2,†} Narendra Sahu,^{3,‡} and Vicky Singh Thounaojam^{3,§}

¹*Department of Physics, Indian Institute of Technology Guwahati, Assam 781039, India*

²*School of Physical Sciences, Indian Institute of Technology Goa, Ponda-403401, Goa, India*

³*Department of Physics, Indian Institute of Technology Hyderabad,
Kandi, Sangareddy 502285, Telangana, India*

Abstract

We study the viability of light thermal dark matter (DM) in sub-GeV mass range in view of the stringent new DAMIC-M limits on DM–electron scattering. Considering a Dirac fermion singlet DM charged under a new Abelian gauge symmetry $U(1)$, we outline two possibilities: (i) family non-universal $U(1)$ gauge coupling with resonantly enhanced DM annihilation into standard model (SM) fermions and (ii) family universal dark $U(1)$ gauge symmetry where relic is set by DM annihilation into light gauge bosons. As an illustrative example of the first class of models, we consider a gauged $L_\mu - L_\tau$ extension of the SM having interesting detection prospects at several experiments. While both of these class of models lead to observed DM relic and consistency with DAMIC-M together with other experimental limits, the second class of models also lead to strong DM self-interactions, potentially solving the small-scale structure issues of cold dark matter. While a vast part of the parameter space in both the models is already ruled out, the current allowed region of parameter space can be further probed at ongoing or future experiments keeping the models testable.

I. INTRODUCTION

The persistent null results from direct-detection experiments [1–3] have shifted considerable attention in the dark matter (DM) community toward exploring the light (sub-GeV) dark matter regime [4–11]. While Weakly Interacting Massive Particles (WIMPs) [12–14] in the GeV–TeV scale had long stood as leading DM candidates, recent experimental advances employing ultra-low threshold detectors have notably improved sensitivity to lighter DM particles [15–21]. Among these, the DAMIC (Dark Matter in CCDs) collaboration, particularly through their most recent DAMIC-M results, has provided the most stringent constraints to date on DM–electron scattering for sub-GeV DM masses [22]. This result, not only significantly improves the direct-detection sensitivity to previously unconstrained ranges but also exclude vast regions of parameter space for a wide class of hidden sector DM models, especially those where DM interactions with the SM particles arise through feeble mixing of a dark sector gauge boson with the photon. In these so-called “Dark Photon” or “Dark gauge-boson” scenarios, the cross-section for DM–electron scattering is highly sensitive to the strength of the kinetic mixing parameter making the latest DAMIC-M bounds crucially relevant for such models.

Recently, sub-GeV DM models which are consistent with the latest DAMIC-M results are studied in Refs. [5, 6]. In [5], the authors derive competitive limits from PandaX-4T S2-only data and surveys their effect on several generic DM models. On the other hand, in [6], the authors perform a status update of thermal DM coupled

to a generic dark photon, arguing that direct-detection results now robustly exclude the complex scalar DM scenario. In this work, we perform a detailed, multi-messenger analysis of two specific, well-motivated sub-GeV DM models; $U(1)_{L_\mu - L_\tau}$ and $U(1)_X$ to demonstrate the survival parameter space which not only satisfy the direct detection results from DAMIC-M, but also satisfy constraints from cosmology, astrophysics, and precision measurements like $(g - 2)_\mu$. We show that, in these models, despite the stringent constraints from DAMIC-M, it is possible to achieve the observed dark matter relic density with phenomenologically viable parameter space consistent with other experimental bounds.

The first scenario we consider is based on a gauged $L_\mu - L_\tau$ extension of the SM [23–25] with family non-universal couplings, motivated not only by its theoretical appeal as an anomaly-free gauge symmetry but also by its experimental verifiability [26, 27]. The $Z_{\mu\tau}$ gauge boson associated with this symmetry is being actively searched for at present and future colliders and fixed-target experiments. Furthermore, this framework is intimately connected to the longstanding discrepancy between the SM and measured value of the anomalous magnetic moment of the muon [28, 29]. While there exists no significant discrepancy between experimental data and updated SM predictions for muon $g - 2$ [30], the latest results from Fermilab [31] can be used to put an upper bound on the $L_\mu - L_\tau$ gauge coupling depending on the gauge boson mass. On the other hand, the flavor-dependent interactions of this model leads to a pronounced suppression of dark matter–electron scattering, as the dominant interactions are with muons and taus. The resulting kinetic mixing with the photon, $\epsilon \sim g_{\mu\tau}/70$, is sufficiently small such that, despite the strong DAMIC-M bounds, the correct relic abundance can be realized through resonant annihilation of DM via the $Z_{\mu\tau}$ portal.

The second scenario we analyze is a generic dark $U(1)_X$ gauge extension with family universal couplings via ki-

*Electronic address: dborah@iitg.ac.in

†Electronic address: satyabrata@iitgoa.ac.in

‡Electronic address: nsahu@phy.iith.ac.in

§Electronic address: ph22resch01004@iith.ac.in

netic mixing of $U(1)_X$ with $U(1)_Y$ of the SM. This construction allows, in principle, more flexibility as the gauge kinetic mixing parameter is now unconstrained and can be treated as a free parameter. Due to the possibility of light gauge boson and relatively larger gauge coupling¹, such a dark $U(1)_X$ extension also allows large DM self-interactions which can address small-scale structure formation issues in cold dark matter (CDM) scenarios such as core-cusp and too-big-to-fail problems [33–35]. When the dual requirements of velocity-dependent DM self-interactions [36–42], and the observed relic density are imposed, viable parameter space gets tightly constrained. In particular, in the regime where dark matter annihilates predominantly into dark gauge bosons to achieve correct relic density, we show that achieving consistency with DAMIC-M and cosmological constraints is possible, but only within tightly restricted corners of the parameter space.

By performing a detailed numerical analysis, we provide a comparative analysis of these two scenarios and identify viable ranges for the DM and mediator masses, couplings, and kinetic mixing where they not only evade the latest direct-detection limits but also satisfy correct relic density as well as all other existing experimental, cosmological and phenomenological constraints. The remainder of this paper is organized as follows. In Sec. II, we present the details of the $U(1)_{L_\mu-L_\tau}$ model, discussing its direct-detection prospects, contribution to the muon anomalous magnetic moment, relic density, and associated constraints, with particular emphasis on how the recent DAMIC-M limits can be consistently satisfied. In Sec. III, we analyze a generic $U(1)_X$ extension, focusing on dark matter direct-detection, self-interactions, relic density, and the corresponding phenomenological limits, again highlighting the regions where DAMIC-M bounds can be accommodated along with other experimental and cosmological constraints. We finally summarize our results and conclude in Sec. IV. Additional technical details, including expressions for self-interaction cross-sections, decay widths, and constraints from N_{eff} , are provided in the Appendices.

II. $U(1)_{L_\mu-L_\tau}$ MODEL

The $U(1)_{L_\mu-L_\tau}$ gauge extension of the SM provides a simple yet well-motivated framework in which the difference of muon and tau lepton numbers is promoted to a local symmetry [23–25]. This construction is particularly attractive because it is anomaly-free without the need for additional fermions, and establishes a natural

connection to neutrino flavor physics. While this model has received lots of attention as an appealing explanation of the previously significant anomaly of muon magnetic moment, in the present scenario, the motivation for this specific framework is primarily due to the suppressed DM-electron couplings that help evade stringent direct-detection bounds from DAMIC-M for sub-GeV DM.

In the minimal setup, the muon and tau leptons (together with their associated neutrinos) carry charges $+1$ and -1 , respectively, under $U(1)_{L_\mu-L_\tau}$. We introduce a SM-singlet Dirac fermion χ as the dark matter candidate with $U(1)_{L_\mu-L_\tau}$ charge q_χ , ensuring anomaly cancellation. The relevant interactions of $U(1)_{L_\mu-L_\tau}$ gauge boson with SM and SM are described by

$$\mathcal{L} \supset -g_{\mu\tau}(Z_{\mu\tau})_\lambda \left(\sum_i q_{f_i} \bar{f}_i \gamma^\lambda f_i \right) - q_\chi g_{\mu\tau} (Z_{\mu\tau})_\lambda \bar{\chi} \gamma^\lambda \chi,$$

where $f_i = \{\mu, \tau, \nu_\mu, \nu_\tau\}$ and the gauge charges are assigned as $q_{f_i} = +1$ for (μ, ν_μ) and $q_{f_i} = -1$ for (τ, ν_τ) . The gauge boson $Z_{\mu\tau}$ acquires its mass $M_{Z_{\mu\tau}}$ through the spontaneous breaking of $U(1)_{L_\mu-L_\tau}$ by an appropriate scalar field. Without any loss of generality we set $q_\chi = 1/2$ which stabilizes the DM without requiring any additional discrete symmetries.

Here, it is important to emphasize that a kinetic mixing term between the SM hypercharge gauge group $U(1)_Y$ and the new $U(1)_{L_\mu-L_\tau}$ can, in general, appear in the Lagrangian, taking the form $\frac{\epsilon}{2} B_{\alpha\beta} Y^{\alpha\beta}$. Here, $B_{\alpha\beta} = \partial_\alpha X_\beta - \partial_\beta X_\alpha$ and $Y_{\alpha\beta}$ denote the field strength tensors of $U(1)_{L_\mu-L_\tau}$ and $U(1)_Y$, respectively, while ϵ is the mixing parameter. Even if this term is absent at the tree level, it is inevitably generated radiatively at one loop through particles carrying charges under both gauge groups. The one-loop mixing is given by [43],

$$\Pi(q^2) = \frac{8eg_{\mu\tau}}{4\pi^2} \int_0^1 dx x(1-x) \ln \left(\frac{m_\tau^2 - x(1-x)q^2}{m_\mu^2 - x(1-x)q^2} \right),$$

which in the limit $q \ll m_\mu$ reduces to

$$\epsilon_A \simeq -\frac{eg_{\mu\tau}}{12\pi^2} \ln \left(\frac{m_\tau^2}{m_\mu^2} \right) \simeq -\frac{g_{\mu\tau}}{70}. \quad (1)$$

Muon Anomalous Magnetic Moment

The longstanding discrepancy between the experimental measurement and the SM prediction of the muon anomalous magnetic moment $a_\mu = (g-2)_\mu/2$ has motivated numerous new physics scenarios. Although the latest lattice-QCD based SM prediction [30] indicates that the tension may no longer be statistically significant, the average of the recent Fermilab measurement [31] with updated SM inputs yields

$$\Delta a_\mu = (39 \pm 64) \times 10^{-11},$$

¹ Self-interacting DM was also studied in the context of gauged $L_\mu - L_\tau$ model by the authors of [32]. But for sub-GeV DM motivated from the recent DAMIC-M results, the experimental constraints on the model parameter space does not allow sufficient self-interactions.

corresponding to a 1σ deviation. In the $U(1)_{L_\mu-L_\tau}$ framework, the new gauge boson $Z_{\mu\tau}$ contributes to this observable at one loop [28, 44, 45],

$$\Delta a_\mu = \frac{g_{\mu\tau}^4}{8\pi^2} \int_0^1 dx \frac{2m_\mu^2 x^2 (1-x)}{x^2 m_\mu^2 + (1-x) M_{Z_{\mu\tau}}^2}. \quad (2)$$

In the present analysis, rather than interpreting this deviation as a genuine anomaly, we employ the Fermilab measurement as an experimental constraint on the parameter space of the model, specifically on the gauge coupling $g_{\mu\tau}$ and the mass of the mediator $M_{Z_{\mu\tau}}$.

Dark Matter Relic Density

For sub-GeV dark matter, achieving the observed relic density via the conventional freeze-out mechanism is typically challenging, since the annihilation cross-section is suppressed and thus insufficient to deplete the dark matter population. In fact, for DM interactions typically in the WIMP ballpark, the requirement of DM not overclosing the Universe leads to a lower bound on its mass, around a few GeV [46, 47]. However, with inclusion of light mediators or additional particles it is possible to realise light thermal DM, as pointed out in several works [11, 48–53]. In the present $U(1)_{L_\mu-L_\tau}$ setup, the process $\chi\bar{\chi} \rightarrow f_i\bar{f}_i$ mediated by the gauge boson $Z_{\mu\tau}$ governs freeze-out, and the tree-level annihilation cross-section takes the form

$$\sigma(s) = \frac{N_{f_i} g_{\mu\tau}^4}{24\pi} \sqrt{\frac{s - 4m_{f_i}^2}{s - 4m_\chi^2}} \frac{s^2 + 2(m_\chi^2 + m_{f_i}^2)s + 4m_{f_i}^2 m_\chi^2}{s[(s - M_{Z_{\mu\tau}}^2)^2 + \Gamma_{Z_{\mu\tau}}^2 M_{Z_{\mu\tau}}^2]}, \quad (3)$$

where $\Gamma_{Z_{\mu\tau}}$ is the total decay width of $Z_{\mu\tau}$ (see Appendix A) and $N_{f_i} = 2$ for charged leptons, while $N_{f_i} = 1$ for neutral leptons. This factor arises due to equal contributions from both left-handed and right-handed chiral components of charged leptons, while for the neutral leptons, there is contribution only from left-handed component. The thermal averaged annihilation cross-section is given by:

$$\langle\sigma v\rangle \simeq \frac{N_{f_i} g_{\mu\tau}^4}{2\pi} \frac{(2m_\chi^2 + m_{f_i}^2)}{(4m_\chi^2 - M_{Z_{\mu\tau}}^2)^2} \sqrt{1 - \frac{m_{f_i}^2}{m_\chi^2}} + \mathcal{O}(v_\chi^2), \quad (4)$$

For $m_\chi, M_{Z_{\mu\tau}} < m_\mu$, the only kinematically open annihilation channels are into neutrinos, making $\chi\chi \rightarrow \bar{\nu}_i\nu_i, i \equiv \mu, \tau$ the dominant contribution. Away from resonance, the cross-section is too small to account for the observed relic density. However, the correct abundance can be achieved near the resonance condition, $M_{Z_{\mu\tau}} \simeq 2m_\chi$, where annihilation is resonantly enhanced. This allows the dark matter population to freeze out with the appropriate relic density without requiring unnaturally large gauge couplings, which are otherwise severely constrained by various experimental searches. While DM

can also annihilate into e^-e^+ final states via one-loop kinetic mixing, it remains suppressed compared to the neutrino final states mentioned above. The same kinetic mixing is also responsible for keeping DM-electron scattering rates below the stringent upper limits set by experiments like DAMIC-M.

Dark Matter direct detection

Direct-detection experiments search for dark matter through its elastic scattering with detector targets, where the interaction deposits a tiny amount of measurable energy in the form of ionization, scintillation or phonon excitations. For dark matter heavier than a few GeV, the dominant channel is scattering off nuclei, producing nuclear recoils. However, for light dark matter in the MeV–GeV range, nuclear recoils are typically below threshold, and the most sensitive probes come instead from DM–electron scattering.

In the present $U(1)_{L_\mu-L_\tau}$ framework, even though DM-electron scattering is suppressed due one-loop kinetic mixing, it can still be constrained from low-threshold experiments such as DAMIC-M and DarkSide-50. The cross-section for elastic DM-electron scattering is given by [54]

$$\sigma_{\chi e} = \frac{\mu_{\chi e}^2}{\pi} \frac{\epsilon_A^2 e^2 g_{\mu\tau}^2}{(M_{Z_{\mu\tau}}^2 + \alpha^2 m_e^2)^2}, \quad (5)$$

where $\mu_{\chi e}$ is the reduced mass of the DM–electron system. This suppression of DM-electron coupling by ϵ_A allows a large portions of the parameter space consistent with relic density requirements to remain viable even under the most recent DAMIC-M and DarkSide-50 constraints.

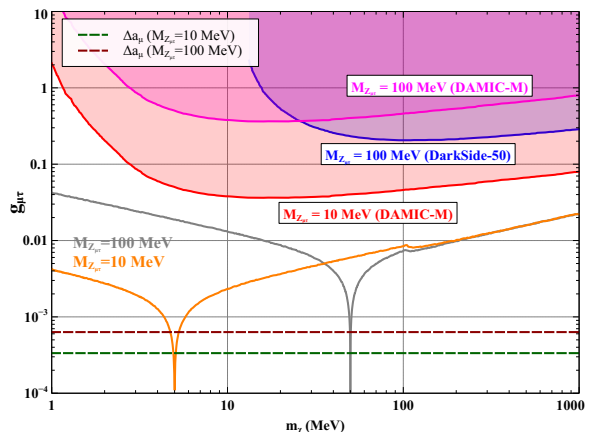


FIG. 1: Relic density favored parameter space in the $(g_{\mu\tau}, m_\chi)$ plane for $M_{Z_{\mu\tau}} = 10$ MeV (orange) and 100 MeV (gray). Direct-detection constraints from DAMIC-M and DarkSide-50, as well as upper limits from $(g-2)_\mu$, are overlaid.

In Fig. 1, we showcase the relic density favored parameter space in the $(g_{\mu\tau}, m_\chi)$ plane for two benchmark mediator masses, $M_{Z_{\mu\tau}} = 10$ MeV (orange) and 100 MeV (gray). Direct-detection limits from DAMIC-M [22] and DarkSide-50 [55] are overlaid, together with the exclusion curve from the muon anomalous magnetic moment $(g-2)_\mu$. A sharp dip in the correct relic density satisfying contour is observed around $m_\chi \simeq M_{Z_{\mu\tau}}/2$, corresponding to the resonance which enhances the cross-section, lowering the required coupling. In this setup, the present $(g-2)_\mu$ constraints are more restrictive than those from direct-detection, such that only parameter points lying in or near the resonant regime remain viable after these constraints are applied.

Indirect detection and CMB constraints

Thermal DM with masses below ~ 20 GeV is subject to severe constraints from the Cosmic Microwave Background (CMB) and indirect-detection searches, as the annihilation cross-sections excluded by these observations lie well below the canonical thermal value required for freeze-out. In this work, we examine the most stringent of these limits by focusing on DM annihilation into e^+e^- final states, which can be used to scrutinize the viable parameter space of the $U(1)_{L_\mu-L_\tau}$ model. Even though the annihilation into electrons is suppressed in this framework due to the loop-induced kinetic mixing parameter $\epsilon_A \sim g_{\mu\tau}/70$, but the resulting bounds still remain very significant.

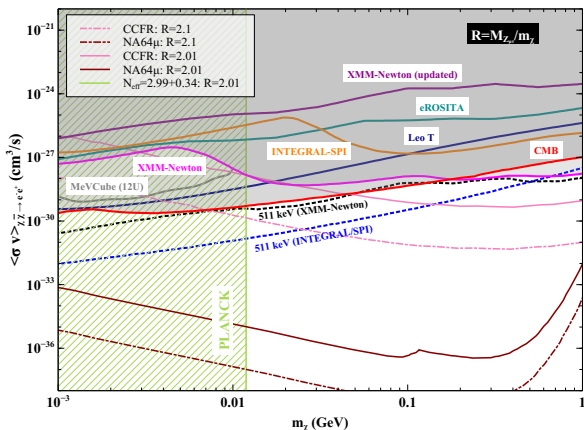


FIG. 2: Indirect-detection limits from X-ray observations constrain the annihilation cross-section $\langle\sigma v\rangle_{\chi\bar{\chi}\to e^+e^-}$. Complementary bounds on the annihilation rate to e^+e^- are plotted by computing the cross-sections for $(R=2.01)$ and $(R=2.1)$ using constraints from fixed-target experiments, specifically CCFR and NA64 μ .

Fig. 2 shows the current bounds on $\langle\sigma v\rangle_{\chi\bar{\chi}\to e^+e^-}$, including the CMB limit from Planck [56, 57] (solid red), as well as indirect search constraints from INTEGRAL-SPI [58] (solid orange), eROSITA [59] (dark cyan), Leo

T [60] (dark blue), MeVCube [61] (solid grey) and XMM-Newton [62] (solid magenta). For completeness, we display both the XMM-Newton bound (magenta) from [62] and the updated bound (dark magenta) reported in [59], where the authors corrected a misapplication of the exposure-weighted solid angle in [62]. Other probes such as AMS-02 and Voyager 1 yield significantly weaker limits compared to Planck and are therefore omitted. In addition to X-ray constraints, we incorporate the bound from the 511 keV emission line [63, 64] from XMM-Newton (black-dotted) and INTEGRAL/SPI (blue dotted), arising from the electron-positron cascade and subsequent positron bound-state formation following DM annihilation to electron-positron pairs. For comparison, we also overlay fixed-target constraints translated from the $(g_{\mu\tau}, M_{Z_{\mu\tau}})$ plane, namely CCFR [65] and NA64 μ [66]. These are shown for representative ratios $R = M_{Z_{\mu\tau}}/m_\chi = 2.01$ (solid) and $R = 2.1$ (dot-dashed), providing complementary bounds to the indirect searches. Astrophysical observations, such as white dwarf cooling, also impose constraints [67] in the $g_{\mu\tau} - M_{Z_{\mu\tau}}$ parameter space. These arise from the unavoidable loop-induced mixing of the $Z_{\mu\tau}$ boson with photon, which enables its decay into electrons and neutrinos, thereby enhancing the stellar cooling rate. However, this constraint remains comparatively weaker than the bounds presented in Fig. 3. We also check for the Indirect search constraints for $\mu^+\mu^-$ final states which is shown in Appendix B.

Other Constraints and Summary

A variety of experimental bounds significantly constrain the parameter space of the $U(1)_{L_\mu-L_\tau}$ model. In Fig. 3, we show the exclusion limits in the $(g_{\mu\tau}, M_{Z_{\mu\tau}})$ plane for two mass ratio $R = M_{Z_{\mu\tau}}/m_\chi = 2.01$ and 2.1. The most stringent limits from direct-detection arise from DM-electron scattering searches, namely DAMIC-M [22] and DarkSide-50 [55], shown by the blue and orange curves, respectively. Additional bounds come from accelerator and neutrino experiments, such as NA64 μ [66], Borexino [68], CCFR [65], COHERENT [69, 70], and BABAR [71], along with the CMB constraint [72] indicated by the brown curve. For comparison, the upper limit of the anomalous magnetic moment deviation of the muon Δa_μ is also displayed by the purple curve. Recent results from NA64 and the updated muon $g-2$ measurements already rule out a large fraction of the parameter space, excluding wide regions of gauge coupling $g_{\mu\tau}$ and mediator mass $M_{Z_{\mu\tau}}$. As expected for s -channel annihilation processes, the CMB constraint provides the strongest bound, as it probes the late-time energy injection from DM annihilations at recombination.

To evade these stringent limits while still accounting for the observed relic abundance, we focus on the resonant annihilation regime, where $m_\chi \simeq M_{Z_{\mu\tau}}/2$. This condition is implemented by fixing $R = 2.01$, and the re-

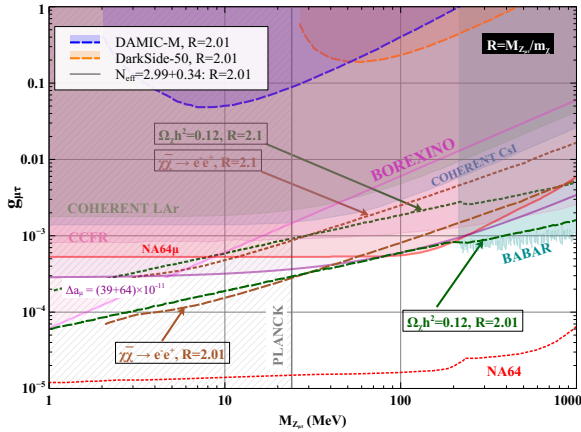


FIG. 3: Constraints in the $(g_{\mu\tau}, M_{Z_{\mu\tau}})$ plane for two representative choices of the mass ratio $R \equiv M_{Z_{\mu\tau}}/m_\chi = 2.01$ (dashed lines) and $R = 2.1$ (dotted lines). The blue (DAMIC-M) and orange (DarkSide-50) curves show direct-detection limits from DM-electron scattering. Additional exclusions from NA64 μ , Borexino, CCFR, COHERENT, BABAR and ΔN_{eff} (PLANCK) are overlaid, along with the CMB bound (brown) shown for both values of R using the corresponding line styles. The dark-green curves denote the parameter space yielding the observed relic abundance for $R = 2.01$ (dashed) and $R = 2.1$ (dotted). As R is increased away from the resonant value $R = 2$, the relic-density contour shifts to larger values of $g_{\mu\tau}$ due to the reduced resonant enhancement. The figure highlights that only a narrow window of $M_{Z_{\mu\tau}}$ remains viable, which will be probed by upcoming NA64 searches.

sulting relic density contour is shown by the dashed green color in Fig. 3. Even under such fine-tuning, we find that viable solutions require $M_{Z_{\mu\tau}} \gtrsim 30$ MeV. At lower mediator masses, the combined CMB and $g-2$ limits entirely exclude the parameter space.

We now briefly comment on the behavior of the relic-density contour with the variation of the ratio $R \equiv M_{Z_{\mu\tau}}/m_\chi$. When R deviates from the resonant value $R = 2$, the s -channel annihilation $\chi\bar{\chi} \rightarrow Z_{\mu\tau} \rightarrow \text{SM}$ moves away from the resonance and a larger gauge coupling $g_{\mu\tau}$ is required to reproduce the canonical thermal cross-section. Hence the relic-density contour shifts to larger $g_{\mu\tau}$ for increasing $|R-2|$. Conversely, as R approaches 2, the resonant enhancement increases the annihilation rate and the required coupling $g_{\mu\tau}$ decreases. For example, with the parameters used in Fig. 3, the relic-density contour lies at smaller values of $g_{\mu\tau}$ for $R = 2.01$ than for $R = 2.1$, and an analogous shift occurs for $R \lesssim 2$, reflecting the symmetric behaviour of the resonance around $R = 2$.

To give a concrete illustration, consider $m_\chi = 50$ MeV. We find that the relic-density contour requires $g_{\mu\tau} \sim 6.3 \times 10^{-4}$ for $R = 2.01$, whereas for $R = 2.1$ the required coupling increases to $g_{\mu\tau} \sim 2 \times 10^{-3}$, pushing the corresponding parameter space into regions already excluded by NA64 μ and the current $(g-2)_\mu$ upper bound. This clearly illustrates that departures from the

near-resonant regime rapidly reduce the viable parameter space.

We also account for constraints from N_{eff} , arising due to modifications in neutrino decoupling or additional contributions to the neutrino energy density from $\chi\bar{\chi}$ annihilation or mediator decays. The details of this analysis are provided in Appendix C. Including these considerations, we find that the gauge boson mass is only viable in a relatively narrow window between ~ 30 MeV and a few hundred MeV. Beyond this range, the parameter space consistent with DM relic density is again excluded, most notably by the BABAR bound. Interestingly, the surviving region lies within the projected sensitivity reach of NA64 [73], implying that the model will be thoroughly tested in the near future.

III. $U(1)_X$ MODEL

Having discussed the loop-induced kinetic mixing in the $U(1)_{L_\mu-L_\tau}$ case, let us now consider a more general extension of the SM with an additional Abelian gauge symmetry $U(1)_X$. Such scenarios are theoretically attractive because they allow additional freedom in model building: in particular, the kinetic mixing parameter ϵ is treated as an independent free parameter, unlike the loop-suppressed mixing in $U(1)_{L_\mu-L_\tau}$. This makes $U(1)_X$ models more flexible in accommodating phenomenological requirements in DM frameworks while retaining a minimal gauge structure.

A generic $U(1)_X$ introduces a new neutral gauge boson X_μ (often denoted Z') that can either couple directly to SM fermions through their assigned $U(1)_X$ charges Q_X^f or indirectly via kinetic mixing with the SM hypercharge boson B_μ :

$$\mathcal{L}_X \supset g_d \sum_f Q_X^f \bar{f} \gamma^\mu f X_\mu - \frac{\epsilon}{2} B_{\mu\nu} X^{\mu\nu}, \quad (6)$$

where the second term induces effective couplings between X_μ and SM fermions even if the latter's $U(1)_X$ charge is zero. We consider this scenario with $Q_X^f = 0$ in the remainder of our discussion.

Through this kinetic mixing, X_μ interacts with the SM fermionic currents as [74]

$$X_\mu j_{\text{SM}}^\mu = -X_\mu \bar{f} \gamma^\mu \{C_L^f P_L + C_R^f P_R\} f, \quad (7)$$

where C_L^f and C_R^f denote the effective left- and right-handed couplings of fermion f to X_μ . These couplings can be expressed in terms of the SM gauge couplings as

$$C_L^f = \left(\sin \eta + \frac{\cos \eta \epsilon s_w}{\sqrt{1-\epsilon^2}} \right) g_L^f - \left(\frac{\cos \eta \epsilon c_w}{\sqrt{1-\epsilon^2}} \right) e Q^f, \quad (8)$$

$$C_R^f = \left(\sin \eta + \frac{\cos \eta \epsilon s_w}{\sqrt{1-\epsilon^2}} \right) g_R^f - \left(\frac{\cos \eta \epsilon c_w}{\sqrt{1-\epsilon^2}} \right) e Q^f,$$

where $s_w = \sin \theta_W$ and $c_w = \cos \theta_W$. The mixing angle η quantifies the mass mixing between the X boson and

the Z boson, given approximately by

$$\tan \eta \simeq \frac{2\epsilon s_w}{1 - \frac{M_X^2}{M_Z^2}}. \quad (9)$$

For reference, the usual SM couplings to Z boson are

$$g_L^f = \frac{g}{c_w} (T_{3L}^f - s_w^2 Q^f), \quad g_R^f = -\frac{g}{c_w} s_w^2 Q^f, \quad (10)$$

where T_{3L}^f and Q^f are the weak isospin and electric charge of fermion f , respectively.

The mass of the new gauge boson X_μ can originate either from the Stueckelberg mechanism [75] or from the Higgs mechanism involving a scalar field charged under the new $U(1)_X$, depending on the specifics of the model construction.

Dark matter self-interactions

Self-interacting dark matter (SIDM) has gained significant attention as a compelling solution to small-scale structure issues in astrophysics. These observations favor dark matter models with sizable self-interaction cross-sections, typically $\sigma/m_\chi \sim 0.1 - 10 \text{ cm}^2/\text{g}$ which can thermalize dark matter within halos and alleviate tensions with collisionless cold dark matter predictions [33–35].

Unlike the $U(1)_{L_\mu-L_\tau}$ model where gauge $g_{\mu\tau} - M_{Z_{\mu\tau}}$ plane is tightly constrained in the sub-GeV regime, a dark $U(1)_X$ allows the possibility of a light gauge boson X_μ together with a relatively strong coupling g_d which can generate the required DM self-interactions via light gauge boson X_μ exchange. Interestingly, DM self-interactions arising via light mediator exchange are velocity-dependent thereby solving the small-scale issues at dwarf galaxy scales while being consistent with standard CDM properties at large or cluster scales [36–40, 42, 76, 77].

The relevant DM Lagrangian is $\mathcal{L} \supset -g_d \bar{\chi} \gamma^\mu \chi X_\mu$, describing dark matter self-interactions mediated by gauge boson X . At non-relativistic velocities, the effective potential for dark matter self-scattering is given by the Yukawa form

$$V(r) = \pm \frac{\alpha_d}{r} e^{-M_X r}, \quad (11)$$

where $\alpha_d = g_d^2/(4\pi)$, and the $-$ sign corresponds to attractive interaction for opposite charges (particle-antiparticle) and the $+$ sign for repulsive interaction for same charges (particle-particle). The detailed expressions for the self-interaction cross-sections are provided in Appendix D.

It should be emphasized that, although the $U(1)_X$ setup offers more freedom compared to the $U(1)_{L_\mu-L_\tau}$ case due to the additional kinetic mixing parameter, the requirement of sizable self-interactions, correct relic density of dark matter and other constraints imposes strong

bounds on the allowed (g_d, m_χ, M_X) parameter space. As a result, the viable region remains highly constrained and hence predictive.

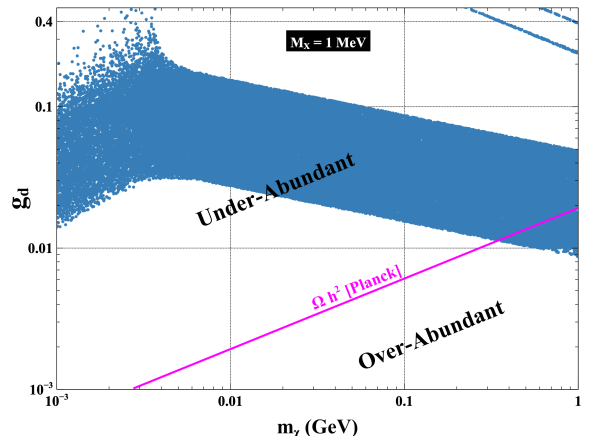


FIG. 4: Parameter space in the g_d - m_χ plane illustrating the region consistent with self-interaction criteria for $M_X = 1 \text{ MeV}$, together with the correct relic density constraint (magenta line) in the minimal setup. Parameter space above the magenta line give an under-abundant relic density, while points below the line are over-abundant. The large blue region indicates the Born-regime of self-interactions while the thin lines in the upper-right corner depicts the transition to the resonant regime (see Appendix D).

Relic Density

In this setup, the relic abundance of dark matter is primarily determined by the annihilation process $\chi\bar{\chi} \rightarrow X^\mu X_\mu$ as opposed to annihilation into SM fermions, since the latter channel is relatively suppressed due to small kinetic mixing [10, 78–81]. This leads to the crucial observation that the relic density calculation is, to leading order, independent of ϵ which instead governs the detection prospects through interactions with visible matter. Even if the small kinetic mixing is insufficient to keep the dark and visible sectors in equilibrium, there exists other portals to do so. For example, in scenarios where the $U(1)_X$ symmetry is broken spontaneously by a scalar S , thermal contact between the dark and visible sectors can still be maintained via the quartic portal interaction $(S^\dagger S)(H^\dagger H)$ with the SM Higgs. By assigning S an appropriate non-trivial $U(1)_X$ charge, its direct Yukawa coupling to DM can be forbidden, thereby leaving the phenomenology discussed here unaffected while ensuring thermal equilibrium at early times.

The thermally averaged annihilation cross-section for dark matter into mediator pairs is s -wave dominated and given by

$$\langle \sigma v \rangle_{\chi\bar{\chi} \rightarrow X X} = \frac{g_d^4}{16\pi m_\chi^2} \sqrt{1 - \frac{M_X^2}{m_\chi^2}}. \quad (12)$$

As a sizable coupling g_d is required to achieve the correct DM self-interactions, this simultaneously enhances the annihilation rate, reducing the relic abundance to the observed range, even for GeV or sub-GeV scale dark matter. This behavior is illustrated in Fig. 4, where the contour of correct relic density is displayed by the solid magenta colored line along with the green shaded region of parameter space consistent with the required DM self-interaction.

Direct detection

Direct detection of dark matter in this framework relies on the small but universal coupling of the X boson to the SM fermions through kinetic mixing. For DM in the 1 MeV–1 GeV mass range, the dominant DM–electron scattering arises due to exchange of X boson.

In the limit of very small ϵ , the induced vector coupling of the X boson to electrons is

$$g_V^e = \frac{C_L^e + C_R^e}{2} \simeq 0.26 \epsilon, \quad (13)$$

which governs the DM–electron scattering process. The corresponding cross-section takes the form

$$\sigma(\chi e \leftrightarrow \chi e) = \frac{\mu_{\chi e}^2}{\pi} \frac{(g_V^e)^2 g_d^2}{(M_X^2 + \alpha^2 m_e^2)^2}, \quad (14)$$

where $\mu_{\chi e}$ is the reduced mass of the DM–electron system.

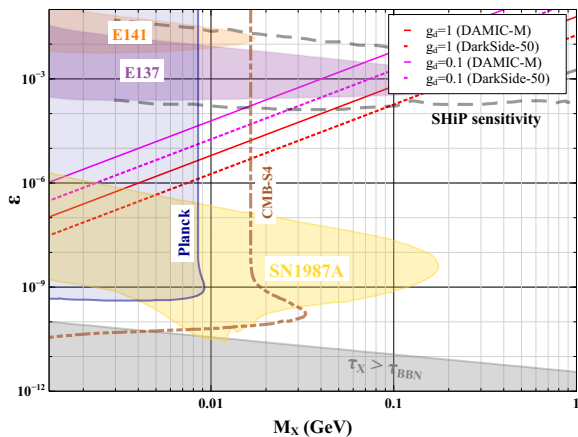


FIG. 5: Parameter space in $\epsilon - M_X$ plane of the $U(1)_X$ model after imposing various constraints. The most stringent bounds from DAMIC-M ($m_\chi=10$ MeV) and DarkSide-50 ($m_\chi=100$ MeV) for two different values of gauge coupling $g_d=$ are shown by solid and dashed lines, respectively. Other shaded regions and contours correspond to different bounds or future sensitivities, see main text for details.

Since the direct-detection cross-section in Eq. (14) depends on the product $\epsilon^2 g_d^2$, the limits from electron recoil searches can be reinterpreted in the $\epsilon - M_X$ parameter

space for given values of g_d . To determine the allowed value of ϵ_{DD} for a given g_d , we use the most sensitive cross-sections from DAMIC-M and DarkSide-50, corresponding to dark matter masses of $m_\chi \sim 10$ MeV and $m_\chi \sim 100$ MeV, respectively. Since for these masses the reduced mass is approximately equal to the electron mass, we obtain the following:

$$\epsilon_{DD} = \begin{cases} 5.508 \times 10^{-5} \left(\frac{0.1}{g_d}\right) \left(\frac{M_X(\text{GeV})}{0.01}\right)^2 & : \text{DAMIC-M} \\ 1.818 \times 10^{-5} \left(\frac{0.1}{g_d}\right) \left(\frac{M_X(\text{GeV})}{0.01}\right)^2 & : \text{DarkSide-50} \end{cases} \quad (15)$$

Eq. 15 gives the most stringent upper bound on the kinetic mixing parameter ϵ from the direct detection experiments DAMIC-M and DarkSide-50. For other dark matter masses, the allowed values of ϵ are larger, with an explicit dependence on m_χ appearing near m_e . This behavior is illustrated in Fig. 5, where we show the strongest constraints from DAMIC-M ($m_\chi = 10$ MeV) and DarkSide-50 ($m_\chi = 100$ MeV) for two representative couplings, $g_d = 0.1$ and $g_d = 1$. The same constraints can be displayed in the σ_e vs m_χ plane for fixed values of M_X and ϵ , highlighting the regions consistent with relic density and self-interaction requirements. The corresponding figure is provided in Appendix E.

Summary of Other Constraints

Fig. 5 also displays existing experimental bounds related to several observables. The purple and orange shaded regions are excluded by electron beam-dump experiments such as SLAC-E141, SLAC-E137 [82, 83], and Fermilab-E774 [84], where dark gauge bosons are produced via Bremsstrahlung processes and subsequently escape detection. The projected sensitivity of the SHiP experiment at CERN [85], designed to probe hidden sectors in conjunction with tau neutrino measurements, is also illustrated. Additionally, the yellow shaded region shows constraints from Supernova 1987A [86], which arise from the requirement that excessive dark gauge boson production should not suppress the observed neutrino flux. Constraints from ΔN_{eff} limit the viable parameter space as well. For mediator masses below 10 MeV, only very small mixings ($\epsilon \lesssim 10^{-9}$) are allowed, as can be seen from the white patch currently allowed by PLANCK, SN1987A and lifetime bounds. On the other hand, for heavier mediators ($M_X > 10$ MeV) the limit weakens to $\epsilon \lesssim 10^{-4}$, as illustrated by the DAMIC-M (solid) and DarkSide-50 (dotted) curves for two specific choices of $g_d = 0.1$ (magenta) and $g_d = 1$ (red). The dot-dashed brown line denotes the sensitivity of the proposed CMB-S4 experiment [87]. Finally, the Big Bang Nucleosynthesis (BBN) bound is also shown, derived by demanding the lifetime of the dark gauge boson X to be shorter than typical BBN timescale.

It is worth noting that in this setup the mediator mass M_X is ideally required to be at or below the MeV scale

or the electron mass threshold, ensuring that it decays exclusively into SM neutrinos. For heavier mediators, one must instead guarantee that X decays dominantly into some form of dark radiation rather than SM charged states. This choice is crucial to evade stringent indirect-detection limits, as well as constraints from CMB measurements on dark matter annihilation into charged final states mediated by X bosons [72, 88–91] of the type $\chi\bar{\chi} \rightarrow XX \rightarrow 4\text{SM}$.

IV. CONCLUSION

In this work, we have analyzed two well-motivated gauge extensions of the Standard Model namely, the gauged $U(1)_{L_\mu-L_\tau}$ and a dark $U(1)_X$ scenario in the context of sub-GeV dark matter which is facing tight constraints from direct-detection experiments like DAMIC-M probing DM-electron scattering. Both the frameworks possess distinctive theoretical and phenomenological appeals and offer viable mechanisms to explain the observed dark matter relic abundance while connecting to broader open questions such as lepton flavor structure, the muon anomalous magnetic moment, and small-scale structure problems of CDM. We have scrutinized these models in light of the latest and significantly improved electron recoil constraints from the DAMIC-M experiment, which severely restrict dark matter–electron scattering cross-sections. Our comprehensive analysis demonstrates that viable regions of parameter space remain in both models which can reproduce the correct relic density while satisfying stringent bounds from direct detection, accelerator searches, cosmology, and astrophysical observations.

The $U(1)_{L_\mu-L_\tau}$ scenario, motivated by its theoretical minimality, anomaly cancellation, and direct connection to the muon $(g-2)$ anomaly, faces increasingly tight constraints from CMB observations, muon anomalous magnetic moment measurements, and accelerator experiments such as NA64. Despite these challenges, a narrow window of parameter space survives due to resonantly enhanced annihilation near $m_\chi \simeq M_{Z_{\mu\tau}}/2$. This near-resonance condition not only permits the observed relic abundance but also keeps the model testable in upcoming experiments, especially NA64 and future low-threshold direct-detection efforts.

In contrast, the generic $U(1)_X$ extension provides additional model-building freedom by treating the kinetic mixing parameter as a free input rather than a loop-induced quantity. A notable and attractive feature of this framework is the decoupling of the process responsible for generating thermal relic from the one determining DM-electron scattering rates. This occurs due to the possibility of dominant DM annihilation into light dark gauge bosons rather than SM fermions, rendering the relic abundance largely independent of the kinetic mixing parameter. Moreover, the presence of a light mediator naturally facilitates velocity-dependent dark matter self-interactions, offering a compelling resolution to

small-scale structure problems that remain unexplained within standard cold dark matter paradigms. Imposing the dual requirements of viable self-interactions and consistency with CMB constraints restricts the viable dark matter mass range to roughly the 300 MeV–1 GeV ballpark, whereas relaxing the self-interaction requirement expands the parameter space considerably.

To conclude, this study points out two interesting ways of realizing sub-GeV thermal DM with a new Abelian gauge interaction which can evade the stringent DAMIC-M constraints on DM-electron scattering. One possibility is to consider family non-universal $U(1)$ gauge charge with resonantly enhanced DM annihilation into SM. Another appealing way is to consider a dark $U(1)$ gauge symmetry with family universal couplings via kinetic mixing where DM dominantly annihilates into light $U(1)$ gauge boson pairs. We considered gauged $L_\mu - L_\tau$ as an illustrative example for the first class of models and compare the sub-GeV DM parameter space with constraints from DAMIC-M, recently updated muon $(g-2)$ world average as well as other bounds from particle physics, cosmology and astrophysics related observations. The second class of models, on the other hand, comes with additional advantage of generating large DM self-interactions potentially solving the small-scale issues of cold DM. A major part of the currently allowed parameter space of both the models remain within reach of future experiments keeping them testable in near future.

Acknowledgments

We are grateful to Shyam Balaji for bringing to our attention the updated experimental bound from XMM-Newton and eROSITA, which has been incorporated in this work. The work of D.B. is supported in part by the Science and Engineering Research Board (SERB), Government of India grant MTR/2022/000575 and the Fulbright-Nehru Academic and Professional Excellence Award 2024-25. We acknowledge helpful conversations with colleagues during the International Conference - Phoenix (2025), which contributed to shaping parts of this study.

Appendix A: Decay Width of a Gauge Boson

The decay width of a gauge boson, say X of $U(1)_X$, to a charged lepton with mass m_f and neutrino, with the corresponding couplings C_L^f, C_R^f and C_L^ν are calculated as

$$\Gamma_{X \rightarrow \nu_i \bar{\nu}_i} = \frac{(C_L^{\nu_i})^2 M_X}{24\pi}, \quad (\text{A1})$$

$$\Gamma_{X \rightarrow f\bar{f}} = \frac{(C_{LR}^f)^2 M_X}{24\pi} \sqrt{1 - \frac{4m_f^2}{M_X^2}}, \quad (\text{A2})$$

where the factor $(C_{LR}^f)^2$ is given by

$$\left((C_L^f)^2 + (C_R^f)^2 \right) \left(1 - \frac{m_f^2}{M_X^2} \right) + 6 \frac{m_f^2}{M_X^2} C_L^f C_R^f. \quad (\text{A3})$$

In the $U(1)_{L_{\mu-L_{\tau}}}$ model, the gauge boson $Z_{\mu\tau}$ has a mass $M_{Z_{\mu\tau}}$, and its couplings to both left- and right-handed fermions are identical, i.e. $C_L^i = C_R^i = C_L^{\nu_i} = g_{\mu\tau}$ where $i = \{\mu, \tau\}$, while for electron, $C_L^e = C_R^e = g_{\mu\tau}/70$.

Appendix B: Indirect Detection

In the $U(1)_{L_{\mu-L_{\tau}}}$ model, for DM masses above the muon threshold, the model permits direct annihilation into $\mu^+\mu^-$. This channel introduces additional constraints from CMB, though they are somewhat weaker compared to those from the electron channel [56, 57] (dotted magenta line in Fig. 6). Fig. 6 presents the corresponding exclusion limits from Planck [57] (red shaded) and XMM-Newton [62] (green shaded), together with the annihilation into e^+e^- (dotted-magenta line) for direct comparison. In the $U(1)_{L_{\mu-L_{\tau}}}$ model, DM annihilation into e^-e^+ channel is suppressed by factor of ϵ_A^2 , in comparison to $\mu^-\mu^+$ channel. Therefore, $\chi\bar{\chi} \rightarrow \mu^+\mu^-$ gives a stronger constraint on $g_{\mu\tau}$ in comparison to $\chi\bar{\chi} \rightarrow e^+e^-$. In other words, the muon final state channel will rule out a larger parameter space on $g_{\mu\tau}$ in comparison to electron final state in Fig 3. The complementary sensitivities projected from fixed-target experiments are also shown, depicted by purple (NA64 μ) and blue (CCFR) curves for $R = 2.1$ (dot-dashed) and $R = 2.01$ (solid).

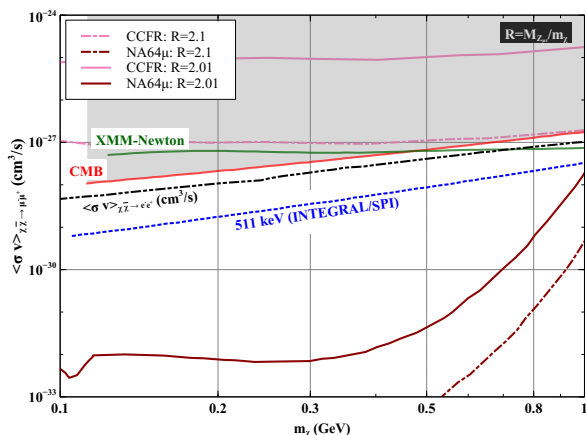


FIG. 6: Indirect detection bounds from DM annihilation into $\mu^+\mu^-$. For DM masses above the muon threshold, the constraint from the $\chi\bar{\chi} \rightarrow e^+e^-$ channel (magenta line) is significantly stronger than that from the $\mu^+\mu^-$ final state (red line).

Appendix C: N_{eff} constraints

If DM mass in the $U(1)_{L_{\mu-L_{\tau}}}$ model is below muon mass threshold m_μ , its annihilation proceeds mainly into neutrinos, allowing us to treat χ and ν as being in thermal equilibrium. For temperatures below the neutrino decoupling temperature, $T_D = 2.3$ MeV, energy injected from DM annihilation increases the total energy density of the neutrino bath. This increase is quantified by N_{eff} , which has a SM value of 3.045 [92–94]. The additional contribution from X -boson decay and DM annihilation can be obtained via entropy conservation and is given by [95]

$$N_{\text{eff}} = N_\nu \left[1 + \frac{1}{N_\nu} \sum_{i=\chi, Z_{\mu\tau}} \frac{g_i}{2} F\left(\frac{m_i}{T_D}\right) \right]^{4/3} \quad (\text{C1})$$

where the function $F(x)$ is given by

$$F(x) = \frac{30}{7\pi^4} \int_x^\infty dy \frac{(4y^2 - x^2)\sqrt{y^2 - x^2}}{e^y \pm 1} \quad (\text{C2})$$

where the $+$ ($-$) sign refers to fermion(boson) statistics.

Fig. 7 depicts the contribution to N_{eff} arising from the decay process $X \rightarrow \nu$, together with the additional contribution from DM annihilation. In the regime $m_\chi > M_{Z_{\mu\tau}}$, the annihilation contribution is negligible, whereas it becomes relevant for $m_\chi < M_{Z_{\mu\tau}}$. The figure also reports the current upper bounds on N_{eff} . Specifically, the 95% C.L. constraint from Planck+lensing+BAO [89] is given by

$$N_{\text{eff}} = 2.99_{-0.33}^{+0.34} \quad (95\%),$$

while a fit including the six Λ CDM parameters extended by N_{eff} and Y_P [89, 96], as presented in [97], yields

$$N_{\text{eff}} = 2.926 \pm 0.286 \quad (95\%).$$

Furthermore, the combination of DESI BAO with CMB data [98] within the one-parameter extension Λ CDM+ N_{eff} provides the constraint

$$N_{\text{eff}} = 3.23_{-0.34}^{+0.35} \quad (95\%).$$

Taken together, these bounds further tighten the parameter space and shift the lower limit on the DM mass inferred from N_{eff} to smaller values.

Appendix D: Low energy cross-sections relevant for the self-interactions of dark matter

Since DM self-interaction is realized due to the presence of the term like $g_d X_\mu \bar{\chi} \gamma^\mu \chi$, the non-relativistic DM

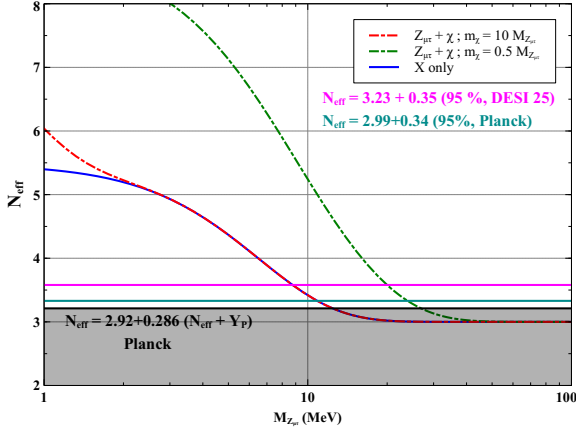


FIG. 7: Contribution to the N_{eff} , arising purely from the $Z_{\mu\tau}$ boson decay (blue), and additional contribution from χ annihilation for two different values of m_χ (dot-dashed red and green lines).

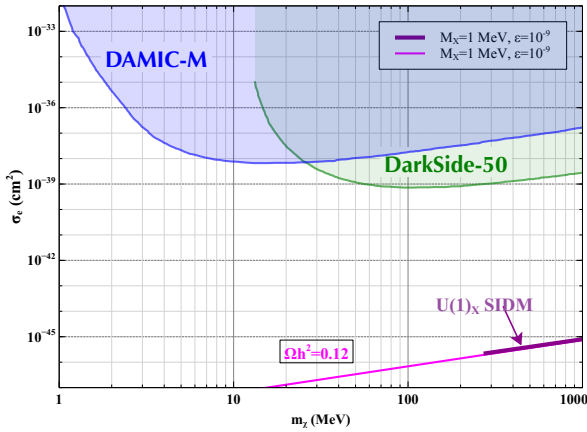


FIG. 8: Parameter space for the correct DM relic density, shown in the σ_{e-m_χ} plane, compared with current bounds from DAMIC-M and DarkSide-50. The magenta line indicates the region consistent with the relic density requirement alone, while the purple line highlights the subset of parameter space that simultaneously satisfies both the relic density and self-interaction constraints.

self-scattering can be well understood in terms of the attractive Yukawa potential

$$V(r) = \pm \frac{g_d^2}{4\pi r} e^{-M_X r} \quad (\text{D1})$$

where the $+$ ($-$) sign denotes repulsive (attractive) potential.

To capture the relevant physics of forward scattering, the transfer cross-section is defined as

$$\sigma_T = \int d\Omega (1 - \cos\theta) \frac{d\sigma}{d\Omega}$$

In the Born limit, $g_d^2 m_\chi / (4\pi M_X) \ll 1$,

$$\sigma_T^{\text{Born}} = \frac{g_d^4}{2\pi m_\chi^2 v_{\text{rel}}^4} \left[\log \left(1 + \frac{m_\chi^2 v_{\text{rel}}^2}{M_X^2} \right) - \frac{m_\chi^2 v_{\text{rel}}^2}{M_X^2 + m_\chi^2 v_{\text{rel}}^2} \right]$$

Outside the Born limit, where $g_d^2 m_\chi / (4\pi M_X) \geq 1$, there can be two different regions: classical regime and resonance regime. In the classical regime ($m_\chi v_{\text{rel}} / M_X \geq 1$), solution for an attractive potential is given by [42, 99, 100]

$$\sigma_T^{\text{class.}} = \begin{cases} \frac{4\pi}{M_X^2} \beta^2 \ln(1 + \beta^{-1}) & \beta \leq 10^{-1} \\ \frac{8\pi}{M_X^2} [\beta^2 / (1 + 1.5\beta^{1.65})] & 10^{-1} < \beta \leq 10^3 \\ \frac{\pi}{M_X^2} [\ln \beta + 1 - 1/2 \ln^{-1} \beta]^2 & \beta \geq 10^3 \end{cases}$$

and for the repulsive potential

$$\sigma_T^{\text{class.}} = \begin{cases} \frac{2\pi}{M_X^2} \beta^2 \ln(1 + \beta^{-2}) & \beta \leq 1 \\ \frac{\pi}{M_X^2} [\ln(2\beta) - \ln(\ln 2\beta)]^2 & \beta \geq 1 \end{cases}$$

where $\beta = \frac{2g_d^2 M_X}{4\pi m_\chi v_{\text{rel}}^2}$.

Finally in the resonance region ($m_\chi v_{\text{rel}} / M_X \leq 1$), no analytical formula for σ_T is available. So approximating the Yukawa potential by Hulthen potential ($V(r) = \pm \frac{g_d^2}{4\pi} \frac{\delta e^{-\delta r}}{1 - e^{-\delta r}}$), the transfer cross-section is obtained to be:

$$\sigma_T^{\text{Hulthen}} = \frac{16\pi \sin^2 \delta_0}{m_\chi^2 v_{\text{rel}}^2}$$

where $l = 0$ phase shift δ_0 is given by:

$$\delta_0 = \text{Arg} \left[\frac{i\Gamma(im_\chi v_{\text{rel}} / \kappa M_X)}{\Gamma(\lambda_+) \Gamma(\lambda_-)} \right]$$

with

$$\lambda_{\pm} = 1 + \frac{im_\chi v_{\text{rel}}}{2\kappa M_X} \pm i^r \sqrt{\frac{g_d^2 m_\chi}{4\pi \kappa M_X} + (-1)^{r+1} \frac{m_\chi^2 v_{\text{rel}}^2}{4\kappa^2 M_X^2}}$$

and $\kappa \approx 1.6$ is a dimensionless number and $r = 0(1)$ for attractive(repulsive) potential.

Appendix E: Direct-detection constraints in the $U(1)_X$ model

Fig. 8 shows direct detection constraints from the DAMIC-M and DarkSide-50 experiments, for DM-electron scattering, indicated by the blue and green contours, respectively. We also explore the parameter space m_χ, g_d consistent with the observed relic density, using $M_X = 1$ MeV and $\epsilon = 10^{-9}$. The resulting cross-sections are shown by the magenta line, with the overlaid purple segment denoting regions that where it is possible

to achieve sufficient DM self-interactions to address the small-scale structure problems of Λ CDM. This illustrates that the relic density–favored parameter space lies well

beyond the sensitivity of current direct detection experiments.

-
- [1] XENON collaboration, *WIMP Dark Matter Search using a 3.1 tonne \times year Exposure of the XENONnT Experiment*, **2502.18005**.
- [2] LZ collaboration, *Dark Matter Search Results from 4.2 Tonne-Years of Exposure of the LUX-ZEPLIN (LZ) Experiment*, **2410.17036**.
- [3] PANDAX collaboration, *Dark Matter Search Results from 1.54 Tonne-Year Exposure of PandaX-4T*, *Phys. Rev. Lett.* **134** (2025) 011805 [2408.00664].
- [4] S. Balan et al., *Resonant or asymmetric: the status of sub-GeV dark matter*, *JCAP* **01** (2025) 053 [2405.17548].
- [5] A. Cheek, P. Figueroa, G. Herrera and I.M. Shoemaker, *Sub-GeV Dark Matter Under Pressure from Direct Detection*, **2507.15956**.
- [6] G. Krnjaic, *Testing Thermal-Relic Dark Matter with a Dark Photon Mediator*, **2505.04626**.
- [7] B. Dutta, S. Ghosh and J. Kumar, *A sub-GeV dark matter model*, *Phys. Rev. D* **100** (2019) 075028 [1905.02692].
- [8] R. Essig, T. Volansky and T.-T. Yu, *New Constraints and Prospects for sub-GeV Dark Matter Scattering off Electrons in Xenon*, *Phys. Rev. D* **96** (2017) 043017 [1703.00910].
- [9] K. Bondarenko, A. Boyarsky, T. Bringmann, M. Hufnagel, K. Schmidt-Hoberg and A. Sokolenko, *Direct detection and complementary constraints for sub-GeV dark matter*, *JHEP* **03** (2020) 118 [1909.08632].
- [10] A. Adhikary, D. Borah, S. Mahapatra, I. Saha, N. Sahu and V.S. Thounaojam, *New realisation of light thermal dark matter with enhanced detection prospects*, *JCAP* **12** (2024) 043 [2405.17564].
- [11] D. Borah, P. Das, S. Mahapatra and N. Sahu, *Light thermal dark matter via type-I seesaw portal*, *JHEP* **08** (2025) 023 [2401.01639].
- [12] G. Bertone, D. Hooper and J. Silk, *Particle dark matter: Evidence, candidates and constraints*, *Phys. Rept.* **405** (2005) 279 [hep-ph/0404175].
- [13] G. Arcadi, M. Dutra, P. Ghosh, M. Lindner, Y. Mambrini, M. Pierre et al., *The waning of the WIMP? A review of models, searches, and constraints*, *Eur. Phys. J. C* **78** (2018) 203 [1703.07364].
- [14] G. Arcadi, D. Cabo-Almeida, M. Dutra, P. Ghosh, M. Lindner, Y. Mambrini et al., *The Waning of the WIMP: Endgame?*, *Eur. Phys. J. C* **85** (2025) 152 [2403.15860].
- [15] XENON collaboration, *Light Dark Matter Search with Ionization Signals in XENON1T*, *Phys. Rev. Lett.* **123** (2019) 251801 [1907.11485].
- [16] CRESST collaboration, *First results from the CRESST-III low-mass dark matter program*, *Phys. Rev. D* **100** (2019) 102002 [1904.00498].
- [17] XENON collaboration, *Search for Light Dark Matter in Low-Energy Ionization Signals from XENONnT*, *Phys. Rev. Lett.* **134** (2025) 161004 [2411.15289].
- [18] PANDAX-II collaboration, *Search for Light Dark Matter-Electron Scatterings in the PandaX-II Experiment*, *Phys. Rev. Lett.* **126** (2021) 211803 [2101.07479].
- [19] PANDAX collaboration, *Search for Light Dark Matter with Ionization Signals in the PandaX-4T Experiment*, *Phys. Rev. Lett.* **130** (2023) 261001 [2212.10067].
- [20] SENSEI collaboration, *SENSEI: Direct-Detection Results on sub-GeV Dark Matter from a New Skipper-CCD*, *Phys. Rev. Lett.* **125** (2020) 171802 [2004.11378].
- [21] SUPERCDMS collaboration, *Light dark matter constraints from SuperCDMS HVeV detectors operated underground with an anticoincidence event selection*, *Phys. Rev. D* **111** (2025) 012006 [2407.08085].
- [22] DAMIC-M collaboration, *Probing Benchmark Models of Hidden-Sector Dark Matter with DAMIC-M*, **2503.14617**.
- [23] R. Foot, *New Physics From Electric Charge Quantization?*, *Mod. Phys. Lett. A* **6** (1991) 527.
- [24] X. He, G.C. Joshi, H. Lew and R. Volkas, *NEW Z-prime PHENOMENOLOGY*, *Phys. Rev. D* **43** (1991) 22.
- [25] X.-G. He, G.C. Joshi, H. Lew and R.R. Volkas, *Simplest Z-prime model*, *Phys. Rev. D* **44** (1991) 2118.
- [26] M. Bauer, P. Foldenauer and J. Jaeckel, *Hunting All the Hidden Photons*, *JHEP* **18** (2020) 094 [1803.05466].
- [27] N. Bernal, J.P. Neto, J. Silva-Malpartida and F.S. Queiroz, *Enabling Thermal Dark Matter within the Vanilla L_μ - L_τ Model*, **2507.02048**.
- [28] S. Baek, N.G. Deshpande, X.G. He and P. Ko, *Muon anomalous $g-2$ and gauged $L(\mu)$ - $L(\tau)$ models*, *Phys. Rev. D* **64** (2001) 055006 [hep-ph/0104141].
- [29] E. Ma, D. Roy and S. Roy, *Gauged $L(\mu)$ - $L(\tau)$ with large muon anomalous magnetic moment and the bimaximal mixing of neutrinos*, *Phys. Lett. B* **525** (2002) 101 [hep-ph/0110146].
- [30] R. Aliberti et al., *The anomalous magnetic moment of the muon in the Standard Model: an update*, **2505.21476**.
- [31] MUON $g-2$ collaboration, *Measurement of the Positive Muon Anomalous Magnetic Moment to 127 ppb*, **2506.03069**.
- [32] A. Kamada, K. Kaneta, K. Yanagi and H.-B. Yu, *Self-interacting dark matter and muon $g-2$ in a gauged $U(1)_{L_\mu-L_\tau}$ model*, *JHEP* **06** (2018) 117 [1805.00651].
- [33] D.N. Spergel and P.J. Steinhardt, *Observational evidence for selfinteracting cold dark matter*, *Phys. Rev. Lett.* **84** (2000) 3760 [astro-ph/9909386].
- [34] S. Tulin and H.-B. Yu, *Dark Matter Self-interactions and Small Scale Structure*, *Phys. Rept.* **730** (2018) 1 [1705.02358].
- [35] J.S. Bullock and M. Boylan-Kolchin, *Small-Scale Challenges to the Λ CDM Paradigm*, *Ann. Rev. Astron.*

- Astrophys.* **55** (2017) 343 [1707.04256].
- [36] M.R. Buckley and P.J. Fox, *Dark Matter Self-Interactions and Light Force Carriers*, *Phys. Rev. D* **81** (2010) 083522 [0911.3898].
- [37] J.L. Feng, M. Kaplinghat and H.-B. Yu, *Halo Shape and Relic Density Exclusions of Sommerfeld-Enhanced Dark Matter Explanations of Cosmic Ray Excesses*, *Phys. Rev. Lett.* **104** (2010) 151301 [0911.0422].
- [38] J.L. Feng, M. Kaplinghat, H. Tu and H.-B. Yu, *Hidden Charged Dark Matter*, *JCAP* **07** (2009) 004 [0905.3039].
- [39] A. Loeb and N. Weiner, *Cores in Dwarf Galaxies from Dark Matter with a Yukawa Potential*, *Phys. Rev. Lett.* **106** (2011) 171302 [1011.6374].
- [40] T. Bringmann, F. Kahlhoefer, K. Schmidt-Hoberg and P. Walia, *Strong constraints on self-interacting dark matter with light mediators*, *Phys. Rev. Lett.* **118** (2017) 141802 [1612.00845].
- [41] M. Kaplinghat, S. Tulin and H.-B. Yu, *Direct Detection Portals for Self-interacting Dark Matter*, *Phys. Rev. D* **89** (2014) 035009 [1310.7945].
- [42] S. Tulin, H.-B. Yu and K.M. Zurek, *Beyond Collisionless Dark Matter: Particle Physics Dynamics for Dark Matter Halo Structure*, *Phys. Rev. D* **87** (2013) 115007 [1302.3898].
- [43] A. Kamada and H.-B. Yu, *Coherent Propagation of PeV Neutrinos and the Dip in the Neutrino Spectrum at IceCube*, *Phys. Rev. D* **92** (2015) 113004 [1504.00711].
- [44] K.R. Lynch, *Extended electroweak interactions and the muon $g - 2$* , *Phys. Rev. D* **65** (2002) 053006 [hep-ph/0108080].
- [45] M. Lindner, M. Platscher and F.S. Queiroz, *A Call for New Physics : The Muon Anomalous Magnetic Moment and Lepton Flavor Violation*, *Phys. Rept.* **731** (2018) 1 [1610.06587].
- [46] B.W. Lee and S. Weinberg, *Cosmological Lower Bound on Heavy Neutrino Masses*, *Phys. Rev. Lett.* **39** (1977) 165.
- [47] E.W. Kolb and K.A. Olive, *The Lee-Weinberg Bound Revisited*, *Phys. Rev. D* **33** (1986) 1202.
- [48] M. Pospelov, A. Ritz and M.B. Voloshin, *Secluded WIMP Dark Matter*, *Phys. Lett. B* **662** (2008) 53 [0711.4866].
- [49] R.T. D’Agnolo and J.T. Ruderman, *Light Dark Matter from Forbidden Channels*, *Phys. Rev. Lett.* **115** (2015) 061301 [1505.07107].
- [50] A. Berlin and N. Blinov, *Thermal Dark Matter Below an MeV*, *Phys. Rev. Lett.* **120** (2018) 021801 [1706.07046].
- [51] R.T. D’Agnolo, D. Liu, J.T. Ruderman and P.-J. Wang, *Forbidden dark matter annihilations into Standard Model particles*, *JHEP* **06** (2021) 103 [2012.11766].
- [52] J. Herms, S. Jana, V.P. K. and S. Saad, *Minimal Realization of Light Thermal Dark Matter*, *Phys. Rev. Lett.* **129** (2022) 091803 [2203.05579].
- [53] C. Jaramillo, *Reviving keV sterile neutrino dark matter*, *JCAP* **10** (2022) 093 [2207.11269].
- [54] R. Essig, M. Fernandez-Serra, J. Mardon, A. Soto, T. Volansky and T.-T. Yu, *Direct Detection of sub-GeV Dark Matter with Semiconductor Targets*, *JHEP* **05** (2016) 046 [1509.01598].
- [55] DARKSIDE collaboration, *Search for Dark Matter Particle Interactions with Electron Final States with DarkSide-50*, *Phys. Rev. Lett.* **130** (2023) 101002 [2207.11968].
- [56] T.R. Slatyer, *Indirect detection of dark matter.*, in *Theoretical Advanced Study Institute in Elementary Particle Physics: Anticipating the Next Discoveries in Particle Physics*, pp. 297–353, 2018, DOI [1710.05137].
- [57] K.E. O’Donnell and T.R. Slatyer, *Constraints on dark matter with future MeV gamma-ray telescopes*, *Phys. Rev. D* **111** (2025) 083037 [2411.00087].
- [58] M. Cirelli, N. Fornengo, B.J. Kavanagh and E. Pinetti, *Integral X-ray constraints on sub-GeV Dark Matter*, *Phys. Rev. D* **103** (2021) 063022 [2007.11493].
- [59] S. Balaji, D. Cleaver, P. De la Torre Luque and M. Michailidis, *Dark Matter in X-rays: Revised XMM-Newton Limits and New Constraints from eROSITA*, **2506.02310**.
- [60] D. Wadekar and Z. Wang, *Strong constraints on decay and annihilation of dark matter from heating of gas-rich dwarf galaxies*, *Phys. Rev. D* **106** (2022) 075007 [2111.08025].
- [61] A.K. Saha, *Searching for dark matter with MeVCube*, *Phys. Rev. D* **111** (2025) 123041 [2501.13162].
- [62] M. Cirelli, N. Fornengo, J. Koechler, E. Pinetti and B.M. Roach, *Putting all the X in one basket: Updated X-ray constraints on sub-GeV Dark Matter*, *JCAP* **07** (2023) 026 [2303.08854].
- [63] P. De la Torre Luque, S. Balaji and J. Silk, *New 511 keV Line Data Provide Strongest sub-GeV Dark Matter Constraints*, *Astrophys. J. Lett.* **973** (2024) L6 [2312.04907].
- [64] D. la Torre Luque; Pedro, S. Balaji, M. Fairbairn, F. Sala and J. Silk, *511 keV galactic photons from a dark matter spike*, *JCAP* **09** (2025) 034 [2410.16379].
- [65] W. Altmannshofer, S. Gori, M. Pospelov and I. Yavin, *Neutrino Trident Production: A Powerful Probe of New Physics with Neutrino Beams*, *Phys. Rev. Lett.* **113** (2014) 091801 [1406.2332].
- [66] NA64 collaboration, *First Results in the Search for Dark Sectors at NA64 with the CERN SPS High Energy Muon Beam*, *Phys. Rev. Lett.* **132** (2024) 211803 [2401.01708].
- [67] P. Foldenauer and J. Hoefken Zink, *How to rule out $(g - 2)_\mu$ in $U(1)_{L_\mu - L_\tau}$ with white dwarf cooling*, *JHEP* **07** (2024) 096 [2405.00094].
- [68] S. Gninenko and D. Gorbunov, *Refining constraints from Borexino measurements on a light Z' -boson coupled to $L_\mu - L_\tau$ current*, *Phys. Lett. B* **823** (2021) 136739 [2007.16098].
- [69] COHERENT collaboration, *Observation of Coherent Elastic Neutrino-Nucleus Scattering*, *Science* **357** (2017) 1123 [1708.01294].
- [70] COHERENT collaboration, *First Measurement of Coherent Elastic Neutrino-Nucleus Scattering on Argon*, *Phys. Rev. Lett.* **126** (2021) 012002 [2003.10630].
- [71] BABAR collaboration, *Search for a muonic dark force at BABAR*, *Phys. Rev. D* **94** (2016) 011102 [1606.03501].
- [72] T.R. Slatyer, *Indirect dark matter signatures in the cosmic dark ages. I. Generalizing the bound on s-wave dark matter annihilation from Planck results*, *Phys. Rev. D* **93** (2016) 023527 [1506.03811].

- [73] S. Gninenko, N. Krasnikov and V. Matveev, *Muon $g-2$ and searches for a new leptophobic sub-GeV dark boson in a missing-energy experiment at CERN*, *Phys. Rev. D* **91** (2015) 095015 [1412.1400].
- [74] D. Borah, S. Mahapatra, N. Sahu and V.S. Thounaojam, *Self-interacting dark matter with observable ΔN_{eff}* , 2504.16910.
- [75] E.C.G. Stueckelberg, *Interaction energy in electrodynamics and in the field theory of nuclear forces*, *Helv. Phys. Acta* **11** (1938) 225.
- [76] M. Kaplinghat, S. Tulin and H.-B. Yu, *Dark Matter Halos as Particle Colliders: Unified Solution to Small-Scale Structure Puzzles from Dwarfs to Clusters*, *Phys. Rev. Lett.* **116** (2016) 041302 [1508.03339].
- [77] L.G. van den Aarssen, T. Bringmann and C. Pfrommer, *Is dark matter with long-range interactions a solution to all small-scale problems of Λ CDM cosmology?*, *Phys. Rev. Lett.* **109** (2012) 231301 [1205.5809].
- [78] D. Borah, S. Mahapatra and N. Sahu, *New realization of light thermal self-interacting dark matter and detection prospects*, *Phys. Rev. D* **108** (2023) L091702 [2211.15703].
- [79] D. Borah, S. Mahapatra, N. Sahu and V.S. Thounaojam, *Self-interacting dark matter and the GRB221009A event*, *Phys. Rev. D* **108** (2023) 083038 [2308.06172].
- [80] S. Mahapatra, S.K. Sahoo, N. Sahu and V.S. Thounaojam, *Self-interacting dark matter and Dirac neutrinos via lepton quarticity*, *Phys. Rev. D* **109** (2024) 055036 [2312.12322].
- [81] D. Borah, S. Mahapatra, P.K. Paul, N. Sahu and P. Shukla, *Asymmetric self-interacting dark matter with a canonical seesaw model*, *Phys. Rev. D* **110** (2024) 035033 [2404.14912].
- [82] J.D. Bjorken, R. Essig, P. Schuster and N. Toro, *New Fixed-Target Experiments to Search for Dark Gauge Forces*, *Phys. Rev. D* **80** (2009) 075018 [0906.0580].
- [83] S. Andreas, C. Niebuhr and A. Ringwald, *New Limits on Hidden Photons from Past Electron Beam Dumps*, *Phys. Rev. D* **86** (2012) 095019 [1209.6083].
- [84] A. Bross, M. Crisler, S. Pordes, J. Volk, S. Errede and J. Wrbanek, *Search for short-lived particles produced in an electron beam dump*, *Phys. Rev. Lett.* **67** (1991) 2942.
- [85] SHiP collaboration, *A facility to Search for Hidden Particles (SHiP) at the CERN SPS*, 1504.04956.
- [86] J.H. Chang, R. Essig and S.D. McDermott, *Revisiting Supernova 1987A Constraints on Dark Photons*, *JHEP* **01** (2017) 107 [1611.03864].
- [87] CMB-S4 collaboration, K.N. Abazajian et al., *CMB-S4 Science Book, First Edition* (10, 2016), 10.2172/1352047, [1610.02743].
- [88] M.S. Madhavacheril, N. Sehgal and T.R. Slatyer, *Current Dark Matter Annihilation Constraints from CMB and Low-Redshift Data*, *Phys. Rev. D* **89** (2014) 103508 [1310.3815].
- [89] PLANCK collaboration, *Planck 2018 results. VI. Cosmological parameters*, *Astron. Astrophys.* **641** (2020) A6 [1807.06209].
- [90] G. Elor, N.L. Rodd, T.R. Slatyer and W. Xue, *Model-Independent Indirect Detection Constraints on Hidden Sector Dark Matter*, *JCAP* **06** (2016) 024 [1511.08787].
- [91] S. Profumo, F.S. Queiroz, J. Silk and C. Siqueira, *Searching for Secluded Dark Matter with H.E.S.S., Fermi-LAT, and Planck*, *JCAP* **03** (2018) 010 [1711.03133].
- [92] G. Mangano, G. Miele, S. Pastor, T. Pinto, O. Pisanti and P.D. Serpico, *Relic neutrino decoupling including flavor oscillations*, *Nucl. Phys. B* **729** (2005) 221 [hep-ph/0506164].
- [93] E. Grohs, G.M. Fuller, C.T. Kishimoto, M.W. Paris and A. Vlasenko, *Neutrino energy transport in weak decoupling and big bang nucleosynthesis*, *Phys. Rev. D* **93** (2016) 083522 [1512.02205].
- [94] P.F. de Salas and S. Pastor, *Relic neutrino decoupling with flavour oscillations revisited*, *JCAP* **1607** (2016) 051 [1606.06986].
- [95] C. Boehm, M.J. Dolan and C. McCabe, *A Lower Bound on the Mass of Cold Thermal Dark Matter from Planck*, *JCAP* **08** (2013) 041 [1303.6270].
- [96] “2018 Planck Explanatory Supplement.” https://wiki.cosmos.esa.int/planck-legacy-archive/index.php/Main_Page.
- [97] C. Giovanetti, M. Lisanti, H. Liu and J.T. Ruderman, *Joint Cosmic Microwave Background and Big Bang Nucleosynthesis Constraints on Light Dark Sectors with Dark Radiation*, *Phys. Rev. Lett.* **129** (2022) 021302 [2109.03246].
- [98] DESI collaboration, *Constraints on Neutrino Physics from DESI DR2 BAO and DR1 Full Shape*, 2503.14744.
- [99] S. Tulin, H.-B. Yu and K.M. Zurek, *Resonant Dark Forces and Small Scale Structure*, *Phys. Rev. Lett.* **110** (2013) 111301 [1210.0900].
- [100] S.A. Khrapak, A.V. Ivlev, G.E. Morfill and S.K. Zhdanov, *Scattering in the attractive yukawa potential in the limit of strong interaction*, *Phys. Rev. Lett.* **90** (2003) 225002.